

General exponential basis set parametrization: Application to time-dependent bivariational wave functions

Mads Greisen Højlund,^{1, a)} Alberto Zocante,^{2, b)} and Ove Christiansen^{1, c)}

¹⁾*Department of Chemistry, University of Aarhus,
Langelandsgade 140, DK-8000 Aarhus C, Denmark*

²⁾*Dipartimento di Scienze e Innovazione Tecnologica, Università del Piemonte
Orientale (UPO), Via T. Michel 11, 15100 Alessandria, Italy*

(Dated: May 8, 2023)

We present equations of motion (EOMs) for general time-dependent wave functions with exponentially parametrized biorthogonal basis sets. The equations are fully bivariational in the sense of the time-dependent bivariational principle (TDBVP) and offer an alternative, constraint free formulation of adaptive basis sets for bivariational wave functions. We simplify the highly non-linear basis set equations using Lie algebraic techniques and show that the computationally intensive parts of the theory are in fact identical to those that arise with linearly parametrized basis sets. Our approach thus offers easy implementation on top of existing code in the context of both nuclear dynamics and time-dependent electronic structure. Computationally tractable working equations are provided for single and double exponential parametrizations of the basis set evolution. The EOMs are generally applicable for any value of the basis set parameters, unlike the approach of transforming the parameters to zero at each evaluation of the EOMs. We show that the basis set equations contain a well-defined set of singularities, which are identified and removed by a simple scheme. The exponential basis set equations are implemented in conjunction with time-dependent vibrational coupled cluster with time-dependent modals (TDMVCC) and we investigate the propagation properties in terms of the average integrator step size. For the systems we test, the exponentially parametrized basis sets yield slightly larger step sizes compared to linearly parametrized basis set.

^{a)}Electronic mail: madsgh@chem.au.dk

^{b)}Electronic mail: alberto.zocante@uniupo.it

^{c)}Electronic mail: ove@chem.au.dk

I. INTRODUCTION

Optimized basis sets are ubiquitous in time-independent quantum chemistry, since the proper choice of basis is crucial to a compact representation of the wave function. The paradigmatic example in electronic structure theory is the self-consistent field (SCF) method, while vibrational SCF (VSCF) plays a similar role in vibrational structure theory. Correlated electronic wave function methods that simultaneously optimize the basis set are also in widespread use, with multi-configurational SCF (MCSCF) as the standard example and density matrix renormalization group (DMRG) with self-consistently optimized orbitals (DMRG-SCF)¹⁻³ as a more recent example. Basis set optimization also plays a role in electronic coupled cluster theory through orthogonal^{4,5} and non-orthogonal⁶ orbital-optimized coupled cluster (OCC and NOCC). These and similar methods require special formal considerations since they are not variational (in the sense of providing an upper bound on the energy) and since the bra and ket states are parametrized in an asymmetric fashion. A principled way of handling this asymmetry while ensuring convergence to full configuration interaction (FCI) is to use the bivariational framework pioneered by Arponen⁷. The NOCC method is fully bivariational and thus converges⁸ to FCI, while OCC does not⁹.

Optimized or adaptive basis sets are also important in explicitly time-dependent theory as illustrated by the success of methods such as multiconfiguration time-dependent Hartree (MCTDH)^{10,11} for nuclear dynamics and the related multiconfiguration time-dependent Hartree-Fock (MCTDHF)^{12,13} for electronic dynamics. Various schemes that use adaptive basis sets (like MCTDH and MCTDHF) but restrict or truncate the wave function expansion are known as well.¹⁴⁻²³ Methods that treat mixed particle types (e.g. fermionic and bosonic) also exist.²⁴⁻²⁷

There has been considerable interest in formulating theories that combine the idea of adaptive basis sets with the use of asymmetric parametrizations such as coupled cluster. Although such theories can be quite involved, several works have appeared in the context of electronic²⁸⁻³⁴ and nuclear^{35,36} dynamics. Some of these works (as well as the present work) utilize Arponen's time-dependent bivariational principle (TDBVP)⁷, which offers a clear formal strategy for deriving equations of motion (EOMs). However, additional work is typically needed to obtain the EOMs in a computationally tractable format and to analyze the EOMs for redundancies and singularities.

It is well known that unitary (invertible) basis set transformations can be parametrized in terms of the exponential of an anti-Hermitian (general) one-particle operator $\hat{\kappa}$ (see Ref. 37 for an overview of the standard mathematical machinery). This constraint free approach results in simple equations when expanding around $\hat{\kappa} = 0$ and has been used frequently in the context of time-independent theory and response theory where one can trivially obtain $\hat{\kappa} = 0$ by absorbing a non-zero $\hat{\kappa}$ into the Hamiltonian integrals. In an explicitly time-dependent context the situation is more complicated and a linear parametrization with constraints has usually been preferred over the exponential parametrization. However, a few exceptions can be found in the literature: Pedersen and Koch³⁸ presented general considerations on exponentially parametrized time-dependent Hartree-Fock (TDHF) but did not derive explicit EOMs for $\hat{\kappa}$. Madsen et al.³⁹ derived and implemented the EOMs for exponentially parametrized time-dependent Hartree (X-TDH) without assuming $\hat{\kappa} = 0$. In this case the exponential parametrization resulted in substantial computational gains compared to the conventional linear parametrization. Recently, Kristiansen et al.³⁴ considered time-dependent OCC and NOCC with double excitations (TDOCCD and TDNOCCD) and introduced the corresponding second-order approximations TDOMP2 and TDNOMP2 with exponentially parametrized orbitals. They used the $\hat{\kappa} = 0$ method to simplify derivations while keeping the benefit of a constraint free formulation. We note that the exponential parametrization with $\hat{\kappa} = 0$ and the linear parametrization with constraints result in very similar working equations although the derivations have different starting points. Allowing $\hat{\kappa} \neq 0$ leads to substantially different equations.

The question of how to parametrize basis sets is not only one of mathematical convenience— it also plays an important role in the propagation of time-dependent wave functions. This includes questions of numerical stability and integrator step size, the latter being a determining factor of the computational cost.

In a recent paper³⁶ we considered linear basis set parametrization and a novel parametrization based on polar decomposition for general time-dependent bivariational wave functions. The purpose of that work was mainly to study the effect on the numerical stability of time-dependent vibrational coupled cluster with time-dependent modals (TDMVCC)³⁵ and it was shown that a so-called restricted polar parametrization offered improved numerical stability compared to the linear parametrization. The present work considers the EOMs for similar kinds of wave functions with exponentially parametrized basis sets without assuming

$\hat{\kappa} = 0$. In addition to the single exponential formalism, we also consider a double exponential basis set parametrization. The former corresponds to the linear parametrization, while the latter parallels the polar parametrization of Ref. 36. The EOMs derived are general with respect to the type of wave function expansion but the main application is coupled cluster theory where a bivariational formulation is natural. We note that the derivations are mainly presented in the language and notation of vibrational structure theory but that all theoretical results carry over to electronic structure theory after minor notational adjustments such as dropping mode indices and sums over modes.

The paper is organized as follows: Section II covers the theory, including a brief introduction to the TDBVP and derivations of EOMs. This is followed by a description of our implementation for the nuclear dynamics case in Sec. III and a few numerical examples in Sec. IV. Section V concludes the paper with a summary of our findings and an outlook on future work.

II. THEORY

A. The time-dependent bivariational principle

Following Arponen⁷, we consider a general bivariational Lagrangian,

$$\mathcal{L} = \langle \Psi' | (i\partial_t - H) | \Psi \rangle, \quad (1)$$

where the bra and ket states are independent. We then determine stationary points ($\delta\mathcal{S} = 0$) of the action-like functional

$$\mathcal{S} = \int_{t_0}^{t_1} \mathcal{L} dt \quad (2)$$

under the condition that the variations of the bra and ket vanish at the endpoints of the integral. In the exact-theory case, a short calculation shows that this procedure is equivalent to the time-dependent Schrödinger equation (TDSE) and its complex conjugate. For approximate, parametrized wave functions, the stationarity condition is instead equivalent to a set of Euler-Lagrange equations (ELEs),

$$0 = \frac{\partial \mathcal{L}}{\partial y_i} - \frac{d}{dt} \frac{\partial \mathcal{L}}{\partial \dot{y}_i}, \quad (3)$$

for all parameters y_i (a short proof of this well-known fact is given in Ref. 36 in a notation consistent with the present work). Writing the Lagrangian as

$$\mathcal{L} = \mathcal{I} - \mathcal{H} \quad (4)$$

with

$$\mathcal{I}(\mathbf{y}, \dot{\mathbf{y}}) = i \langle \Psi' | \dot{\Psi} \rangle = i \sum_j \dot{y}_j \left\langle \Psi' \left| \frac{\partial \Psi}{\partial y_j} \right. \right\rangle, \quad (5a)$$

$$\mathcal{H}(\mathbf{y}, t) = \langle \Psi' | H | \Psi \rangle, \quad (5b)$$

the ELEs in Eq. (3) become

$$\frac{\partial \mathcal{I}}{\partial y_i} - \frac{d}{dt} \frac{\partial \mathcal{I}}{\partial \dot{y}_i} = \frac{\partial \mathcal{H}}{\partial y_i}. \quad (6)$$

After carrying out the derivatives using the chain and product rules and cancelling terms, one gets the following appealing EOMs:

$$i \sum_j \mathcal{M}_{ij} \dot{y}_j = \frac{\partial \mathcal{H}}{\partial y_i}. \quad (7)$$

Here, we have defined an anti-symmetric matrix \mathcal{M} with elements

$$\mathcal{M}_{ij} = \left\langle \frac{\partial \Psi'}{\partial y_i} \left| \frac{\partial \Psi}{\partial y_j} \right. \right\rangle - \left\langle \frac{\partial \Psi'}{\partial y_j} \left| \frac{\partial \Psi}{\partial y_i} \right. \right\rangle. \quad (8)$$

The EOMs in Eq. (7) constitute a natural bivariational analogue of the general variational EOMs considered by e.g. Kramer and Saraceno⁴⁰ and Ohta⁴¹.

B. Parametrization

We will consider general wave function parametrizations of the form

$$|\Psi(\boldsymbol{\alpha}, \boldsymbol{\kappa})\rangle = e^{\hat{\kappa}} |\psi(\boldsymbol{\alpha})\rangle \quad (9a)$$

$$\langle \Psi'(\boldsymbol{\alpha}, \boldsymbol{\kappa}) | = \langle \psi'(\boldsymbol{\alpha}) | e^{-\hat{\kappa}} \quad (9b)$$

where the one-particle operator $\hat{\kappa}$ generates invertible linear transformations of the basis functions (modals or orbitals). In the vibrational case, we use the notation of many-mode second quantization⁴² and write

$$\hat{\kappa} = \sum_m \sum_{p^m q^m} \kappa_{p^m q^m}^m E_{p^m q^m}^m. \quad (10)$$

The parameters $\kappa_{p^m q^m}^m$ are collected in vectors $\boldsymbol{\kappa}^m$ or matrices \mathbf{K}^m depending on context. The one-mode shift operators,

$$E_{p^m q^m}^m = a_{p^m}^{m\dagger} b_{q^m}^m, \quad (11)$$

satisfy the commutator

$$[E_{p^m q^m}^m, E_{r^m s^m}^{m'}] = \delta_{mm'} (\delta_{q^m r^m} E_{p^m s^m}^m - \delta_{p^m s^m} E_{r^m q^m}^m) \quad (12)$$

and constitute the generators of the general linear group. The well-known one-electron shift operators satisfy essentially the same commutator³⁷, which means that the derivations in this work carry over to electronic structure theory after removing mode indices as appropriate. We will denote the remaining wave function parameters $\boldsymbol{\alpha}$ as configurational parameters. The non-transformed states $|\psi(\boldsymbol{\alpha})\rangle$ and $\langle\psi'(\boldsymbol{\alpha})|$ are assumed to be expressed in the same primitive basis as the $\hat{\kappa}$ operator. We will allow for the case where the wave function is expanded in an active subset of the primitive basis. In Sec. **II C** we simply require that the primitive basis is biorthonormal, while we require orthonormality in Sec. **II F**. We note that this restriction can likely be lifted with appropriate modifications of the derivations.

C. Equations of motion

Ordering the parameters like $\mathbf{y} = (\boldsymbol{\alpha}, \boldsymbol{\kappa})$, the EOMs in Eq. (7) assume the structure

$$i \left[\begin{array}{c|c} \mathbf{M} & \tilde{\mathbf{A}} \\ \hline -\tilde{\mathbf{A}}^\top & \tilde{\mathbf{C}} \end{array} \right] \begin{bmatrix} \dot{\boldsymbol{\alpha}} \\ \dot{\boldsymbol{\kappa}} \end{bmatrix} = \begin{bmatrix} \mathbf{h} \\ \tilde{\mathbf{f}} \end{bmatrix}. \quad (13)$$

The various matrix elements can be calculated by direct application of Eq. (8) followed by the appropriate use of

$$e^{\hat{\kappa}} e^{-\hat{\kappa}} = 1, \quad (14a)$$

$$\frac{\partial e^{-\hat{\kappa}}}{\partial \kappa_{p^m q^m}^m} e^{\hat{\kappa}} = -e^{-\hat{\kappa}} \frac{\partial e^{\hat{\kappa}}}{\partial \kappa_{p^m q^m}^m} \quad (14b)$$

where the latter follows from taking the derivative of the former. For notational convenience, we define a similarity transformed derivative^{43,44}

$$\begin{aligned}
D_{p^m q^m}^m &= e^{-\hat{\kappa}} \frac{\partial e^{\hat{\kappa}}}{\partial \kappa_{p^m q^m}^m} \\
&= e^{-\hat{\kappa}^m} \frac{\partial e^{\hat{\kappa}^m}}{\partial \kappa_{p^m q^m}^m} \\
&= \sum_{n=0}^{\infty} \frac{(-1)^n}{(n+1)!} (\text{ad}_{\hat{\kappa}^m})^n E_{p^m q^m}^m \\
&= \sum_{r^m s^m} d_{(p^m q^m)(r^m s^m)}^m E_{r^m s^m}^m
\end{aligned} \tag{15}$$

with $\text{ad}_{\hat{\kappa}^m}(X) = [\hat{\kappa}^m, X]$ (the second equality follows from the fact that $[\hat{\kappa}^m, \hat{\kappa}^{m'}] = 0$ for $m \neq m'$). This operator is a one-particle operator as indicated by the last equality in Eq. (15). For now we assume that the matrix elements $d_{(p^m q^m)(r^m s^m)}^m$ are available and collect them in a matrix \mathbf{D}^m . We will later show how the elements of \mathbf{D}^m can be calculated and, in particular, how transformations by \mathbf{D}^m can be performed in an efficient manner without explicitly constructing the full matrix. The matrix elements needed for Eq. (13) are now given by

$$M_{ij} = \left\langle \frac{\partial \psi'}{\partial \alpha_i} \middle| \frac{\partial \psi}{\partial \alpha_j} \right\rangle - \left\langle \frac{\partial \psi'}{\partial \alpha_j} \middle| \frac{\partial \psi}{\partial \alpha_i} \right\rangle \tag{16a}$$

$$\tilde{A}_{i(m'r^m s^m)} = \frac{\partial}{\partial \alpha_i} \langle \psi' | D_{r^m s^m}^{m'} | \psi \rangle \tag{16b}$$

$$\tilde{C}_{(m p^m q^m)(m' r^m s^m)} = \langle \psi' | [D_{r^m s^m}^{m'}, D_{p^m q^m}^m] | \psi \rangle \tag{16c}$$

$$h_i = \frac{\partial}{\partial \alpha_i} \langle \psi' | \bar{H} | \psi \rangle \tag{16d}$$

$$\tilde{f}_{(m p^m q^m)} = \langle \psi' | [\bar{H}, D_{p^m q^m}^m] | \psi \rangle \tag{16e}$$

where we have defined

$$\bar{H} = e^{-\hat{\kappa}} H e^{\hat{\kappa}} \tag{17}$$

and used a tilde to indicate the quantities that depend on the $D_{p^m q^m}^m$ operators. These quantities can be quite complicated since $D_{p^m q^m}^m$ is generally a full one-particle operator. In particular, one cannot immediately analyze the elements of $\tilde{\mathbf{A}}$ and $\tilde{\mathbf{C}}$ for zeros. Having calculated the matrix elements of the EOMs, it is easy to show that Eq. (13) is equivalent to

$$i\dot{\boldsymbol{\alpha}} = \mathbf{M}^{-1}(\mathbf{h} - i\tilde{\mathbf{A}}\dot{\boldsymbol{\kappa}}), \tag{18a}$$

$$i(\tilde{\mathbf{C}} + \tilde{\mathbf{A}}^T \mathbf{M}^{-1} \tilde{\mathbf{A}})\dot{\boldsymbol{\kappa}} = \tilde{\mathbf{f}} + \tilde{\mathbf{A}}^T \mathbf{M}^{-1} \mathbf{h}. \tag{18b}$$

if \mathbf{M} is invertible. The \mathbf{M} matrix is usually rather trivial in a way that does not depend on the concrete parameter values but rather on the type of parametrization. Two examples (coupled cluster and linearly expanded wave functions) are given in Ref. 36. In those cases, the \mathbf{M} matrix and its inverse are simply given by

$$\mathbf{M} = \left[\begin{array}{c|c} \mathbf{0} & -\mathbf{1} \\ \hline +\mathbf{1} & \mathbf{0} \end{array} \right], \quad \mathbf{M}^{-1} = \left[\begin{array}{c|c} \mathbf{0} & +\mathbf{1} \\ \hline -\mathbf{1} & \mathbf{0} \end{array} \right]. \quad (19)$$

For extended coupled cluster, the \mathbf{M} matrix is not trivial but it can still be inverted analytically and without singularities.⁴⁵ We are currently not aware of any wave function where \mathbf{M} can become singular. Instead, the main difficulty is that Eq. (18b) cannot generally (i.e. for $\hat{\kappa} \neq 0$) be solved as it stands due to the presence of redundancies that do not simply consist of certain blocks being equal to zero. We can circumvent this problem by introducing appropriate zeroth order quantities, i.e.

$$A_{i(m'r'm's'm')} = \frac{\partial}{\partial \alpha_i} \langle \psi' | E_{r'm's'm'}^{m'} | \psi \rangle, \quad (20a)$$

$$C_{(m p^m q^m)(m'r'm's'm')} = \langle \psi' | [E_{r'm's'm'}^{m'}, E_{p^m q^m}^m] | \psi \rangle, \quad (20b)$$

$$f_{(m p^m q^m)} = \langle \psi' | [\bar{H}, E_{p^m q^m}^m] | \psi \rangle. \quad (20c)$$

These are simpler to calculate and, more importantly, allow a straight-forward (although possibly tedious) identification of vanishing matrix elements through analysis of the shift operator expressions. The introduction of a block-diagonal matrix \mathbf{D} with elements

$$d_{(m p^m q^m)(m'r'm's'm')} = \delta_{mm'} d_{(p^m q^m)(r^m s^m)}^m \quad (21)$$

now allows us to write

$$\tilde{\mathbf{A}} = \mathbf{A} \mathbf{D}^T, \quad (22a)$$

$$\tilde{\mathbf{C}} = \mathbf{D} \mathbf{C} \mathbf{D}^T, \quad (22b)$$

$$\tilde{\mathbf{f}} = \mathbf{D} \mathbf{f}, \quad (22c)$$

thus relating the simple zeroth order matrices to the infinite order matrices. Substituting Eqs. (22) into Eqs. (18) then yields

$$i \dot{\boldsymbol{\alpha}} = \mathbf{M}^{-1} (\mathbf{h} - i \mathbf{A} \mathbf{D}^T \dot{\boldsymbol{\kappa}}), \quad (23a)$$

$$i \mathbf{D} (\mathbf{C} + \mathbf{A}^T \mathbf{M}^{-1} \mathbf{A}) \mathbf{D}^T \dot{\boldsymbol{\kappa}} = \mathbf{D} (\mathbf{f} + \mathbf{A}^T \mathbf{M}^{-1} \mathbf{h}). \quad (23b)$$

These equations are further simplified by removing \mathbf{D} on both sides of Eq. (23b) and introducing the definition

$$\mathbf{g} = i\mathbf{D}^\top \dot{\boldsymbol{\kappa}} \quad (24)$$

in order to write

$$i\dot{\boldsymbol{\alpha}} = \mathbf{M}^{-1}(\mathbf{h} - \mathbf{A}\mathbf{g}), \quad (25a)$$

$$(\mathbf{C} + \mathbf{A}^\top \mathbf{M}^{-1} \mathbf{A})\mathbf{g} = (\mathbf{f} + \mathbf{A}^\top \mathbf{M}^{-1} \mathbf{h}). \quad (25b)$$

Equations (25) are the central equations of the present work and determine the time evolution of the parameters. Equation (25a) directly gives the time derivative of the configurational parameters, while Eq. (25b) determines the evolution of the basis set parameters in a slightly indirect way: First the equation is solved, and then $\dot{\boldsymbol{\kappa}}$ is recovered from Eq. (24). In the general case, this involves the inversion of \mathbf{D}^\top , while the computation reduces to $\dot{\boldsymbol{\kappa}} = -i\mathbf{g}$ in the $\hat{\kappa} = 0$ case. It is interesting to note that Eqs. (25) are in fact *identical* to the central equations for bivariational wave functions with linearly parametrized basis sets [Eqs. (46) and (63) in Ref. 36]. In that work, Eq. (25b) appeared as a consequence of the necessary biorthonormality constraints and it was shown how it can be analyzed for redundancies and solved for relevant types of wave functions, e.g. coupled cluster. The important point here is that the central and computationally intensive equations are *independent* of the choice of basis set parametrization.

As a final simplification we define

$$\mathbf{h}' = \mathbf{h} - \mathbf{A}\mathbf{g} \quad (26)$$

and write the configurational EOMs compactly as

$$i\dot{\boldsymbol{\alpha}} = \mathbf{M}^{-1}\mathbf{h}'. \quad (27)$$

According to Eqs. (16d) and (20a) one may calculate the elements of \mathbf{h}' as

$$h'_i = \frac{\partial}{\partial \alpha_i} \langle \psi' | (\bar{H} - \hat{g}) | \psi \rangle = \frac{\partial \mathcal{H}'}{\partial \alpha_i} \quad (28)$$

with the one-particle operator \hat{g} and the modified Hamiltonian function \mathcal{H}' given by

$$\hat{g} = \sum_m \sum_{p^m q^m} g_{p^m q^m}^m E_{p^m q^m}^m, \quad (29)$$

$$\mathcal{H}' = \langle \psi' | (\bar{H} - \hat{g}) | \psi \rangle. \quad (30)$$

Assuming that we are able to solve Eq. (25b) for \mathbf{g} , we need to recover $\dot{\boldsymbol{\kappa}}$ in order to integrate the EOMs. Using the definition in Eq. (24) and taking \mathbf{D}^\top to be invertible, this means that we should compute

$$\dot{\boldsymbol{\kappa}}^m = -i(\mathbf{D}^m)^{-\top} \mathbf{g}^m \quad (31)$$

for each mode. Doing this efficiently requires some general considerations on similarity transformed derivatives such as the one in Eq. (15). These considerations are covered by the next section.

D. Similarity transformed derivative

In this section, we leave the notation of the main text and consider a general Lie group. We note that the following derivations are rather generic in a Lie group context but we give the details for the convenience of the reader. Somewhat similar considerations (although considerably less general) can be found in Exercise 3.5 of Ref. 37.

The generators of the group (i.e. the basis of the Lie algebra) will be denoted by E_i where i might be a compound index. An element X of the Lie algebra can then be written as

$$X = X_i E_i \quad (32)$$

where repeated indices imply summation (this convention is used throughout this section). The Lie algebra is characterized by the commutators (Lie brackets)

$$[E_i, E_j] = f_{ij}^k E_k \quad (33)$$

where the scalars f_{ij}^k are denoted structure constants. Equation (33) is completely general and covers, e.g., the one-particle shift operator commutator in Eq. (12). We will consider the case where X depends on a parameter s through the coefficients X_i and compute the quantity⁴³

$$D = e^{-X(s)} \frac{d}{ds} e^{X(s)} = \sum_{k=0}^{\infty} \frac{(-1)^k}{(k+1)!} (\text{ad}_X)^k \dot{X} \quad (34)$$

where

$$\text{ad}_X(Y) = [X, Y], \quad (35)$$

$$\dot{X} = \frac{dX}{ds} = \frac{dX_i}{ds} E_i = \dot{X}_i E_i. \quad (36)$$

Before proceeding we note that

$$[X, E_i] = X_j [E_j, E_i] = X_j f_{ji}^k E_k = Q_{ik} E_k \quad (37)$$

where we have defined a matrix \mathbf{Q} with elements

$$Q_{ik} = X_j f_{ji}^k. \quad (38)$$

Equation (37) simply shows that commutation by X translates to contraction with the matrix \mathbf{Q} . Using this fact, the first few commutators in the expansion become

$$\begin{aligned} (\text{ad}_X)^0 \dot{X} &= \dot{X}_i E_i \\ &= \dot{X}_i (\mathbf{Q}^0)_{ij} E_j, \end{aligned} \quad (39a)$$

$$\begin{aligned} (\text{ad}_X)^1 \dot{X} &= [X, \dot{X}_i E_i] \\ &= \dot{X}_i (\mathbf{Q}^1)_{ij} E_j, \end{aligned} \quad (39b)$$

$$\begin{aligned} (\text{ad}_X)^2 \dot{X} &= [X, [X, \dot{X}_i E_i]] \\ &= \dot{X}_i (\mathbf{Q}^2)_{ij} E_j, \end{aligned} \quad (39c)$$

⋮

Combining this pattern with Eq. (34) yields an attractive expression, namely

$$D = \dot{X}_i \left[\sum_{k=0}^{\infty} \frac{(-1)^k}{(k+1)!} \mathbf{Q}^k \right]_{ij} E_j \equiv \dot{X}_i d_{ij} E_j. \quad (40)$$

We collect the elements d_{ij} in a matrix \mathbf{D} . This matrix encodes the structure of the Lie algebra (through the structure constants) and the information tied to the specific element X and provides, in essence, a local basis for expressing D directly in terms of the generators.

If we choose $s = X_k$, then it must be the case that $\dot{X}_i = \delta_{ki}$ and the equation above simplifies to

$$D = d_{kj} E_j \quad (41)$$

In this case, we see that the \mathbf{D} matrix simply contains the expansion coefficients for the operator D . In order to compute \mathbf{D} , we assume that \mathbf{Q} is diagonalizable as $\mathbf{Q} = \mathbf{P}\mathbf{\Lambda}\mathbf{P}^{-1}$ and write

$$\mathbf{D} = \mathbf{P}\varphi(\mathbf{\Lambda})\mathbf{P}^{-1} \quad (42)$$

where the function

$$\varphi(z) = \sum_{k=0}^{\infty} \frac{(-1)^k}{(k+1)!} z^k = \begin{cases} \frac{1 - \exp(-z)}{z} & \text{if } z \neq 0 \\ 1 & \text{if } z = 0 \end{cases} \quad (43)$$

is applied to the diagonal elements λ_i of \mathbf{A} , i.e. to the eigenvalues of \mathbf{Q} . We have used the limit $\varphi(z) \rightarrow 1$ as $z \rightarrow 0$ to define $\varphi(0)$. Looking at Eq. (42) it is evident that \mathbf{D} has eigenvalues $\varphi(\lambda_i)$. This implies that \mathbf{D} is invertible when $\varphi(\lambda_i) \neq 0$, i.e. when $\lambda_i \neq 2\pi ik$ where k is a non-zero integer.

E. Simplified equations of motion

Section IID provides a feasible and very general procedure for computing the \mathbf{D}^m matrices. However, it is not at all obvious that this procedure will lead to efficient working equations. In Appendix A we work out the details and show that an attractive result can indeed be obtained provided the matrix \mathbf{K}^m (which holds the elements of the vector $\boldsymbol{\kappa}^m$) is diagonalizable. Dropping the mode index for clarity, we assume that

$$\mathbf{K} = \mathbf{R}\boldsymbol{\mu}\mathbf{L}^\dagger, \quad \mathbf{L}^\dagger\mathbf{R} = \mathbf{R}\mathbf{L}^\dagger = \mathbf{1} \quad (44)$$

where $\boldsymbol{\mu}$ is diagonal and construct an auxiliary matrix $\boldsymbol{\Omega}$ with elements

$$\omega_{pq} = 1/\varphi(\mu_p - \mu_q). \quad (45)$$

The numbers $\varphi(\mu_p - \mu_q)$ are in fact the eigenvalues of \mathbf{D}^\top and our assumption that \mathbf{D}^\top is invertible is equivalent to assuming

$$\varphi(\mu_p - \mu_q) \neq 0 \quad \iff \quad \mu_p - \mu_q \neq 2\pi ik \quad (46)$$

where k is a non-zero integer. With these prerequisites in place, the result is given by

$$\dot{\mathbf{K}} = -i\mathbf{R}(\boldsymbol{\Omega} \circ (\mathbf{L}^\dagger\mathbf{G}\mathbf{R}))\mathbf{L}^\dagger \quad (47)$$

where $\dot{\mathbf{K}}$ and \mathbf{G} are the matrices holding the elements of the vectors $\dot{\boldsymbol{\kappa}}$ and \mathbf{g} , respectively, for each mode (see Appendix A for details). The symbol \circ denotes the Hadamard (or element-wise) product. Although the transformation in Eq. (47) may look somewhat unusual, it is not expensive to perform and can be easily implemented.

In summary, the steps necessary for the exponential parametrization are as follows: (i) solve Eq. (25b) to obtain \mathbf{G} ; (ii) diagonalize \mathbf{K} as in Eq. (44); (iii) compute $\mathbf{\Omega}$ using Eq. (45); and (iv) obtain $\dot{\mathbf{K}}$ from Eq. (47). Regarding the computational cost, we note that the diagonalization step scales as $\mathcal{O}(N^3)$, where N is the dimension of \mathbf{K} , i.e. the number of basis functions. The computation of Eq. (47) involves $4N^3 + N^2$ multiplications if the matrix and Hadamard products are done sequentially. In total, the computational cost arising from the exponential parametrization scales as $\mathcal{O}(N^3)$ (keeping only the leading term).

In the vibrational case, the diagonalization of \mathbf{K} and computation of Eq. (47) is performed separately for each mode so the cost is $\mathcal{O}(MN^3)$, where M is the number of modes and N is the number of basis functions per mode. It is important to note that N does not scale with the size of the system, so the additional steps involved in the exponential parametrization have a cost that is simply linear in M . This cost can safely be considered negligible.

For electrons, the number of basis functions does scale with the size of the system so the cost is not negligible as such. In addition, N may conceivably be very large (e.g. in the case of grid-based methods) so that diagonalization of \mathbf{K} is not realistic. In cases where the diagonalization is feasible, the $\mathcal{O}(N^3)$ scaling is often much lower than the scaling arising from the wave function expansion and from integral transformations. In those cases, the operations related to the basis set parametrization are not decisive for the cost of evaluating the full set of EOMs.

Finally, it should be recalled that the most important computational difference between various choices of basis set parametrization may derive from the performance of the numerical integration, i.e. from the number of EOM evaluations. For a given choice of integration algorithm, this number is determined by the average integrator step size, which we will consider in Sec. IV.

F. Double exponential parametrization

For each mode we may choose to parametrize the basis functions in terms of the unique polar decomposition⁴³,

$$e^{\hat{\kappa}} = e^{\hat{\kappa}'} e^{\hat{\kappa}''} \quad (48)$$

where $\hat{\kappa}'$ is anti-Hermitian and $\hat{\kappa}''$ is Hermitian (we have dropped the mode index for clarity). These properties imply that $e^{\hat{\kappa}'}$ is unitary while $e^{\hat{\kappa}''}$ is positive definite (i.e. Hermitian with

strictly positive eigenvalues). We note that double exponential orbital transformations have been considered by Olsen⁴⁶ in the context of ground state configuration interaction (CI) calculations with non-orthogonal orbitals.

In order to motivate such a parametrization we need to consider the situation where the basis set is divided into active and secondary subsets, with the wave function being expanded in the active basis alone. The exponential parametrization employed in the present work ensures that the bra basis functions (given by $e^{-\hat{\kappa}}$) and the ket basis functions (given by $e^{\hat{\kappa}}$) are biorthonormal by construction. Specifically, the active bra and ket functions are biorthonormal. However, there is no guarantee that they span the same space. Although this situation is allowed by the formalism, we have found³⁶ that the active bra and ket basis functions sometimes tend to drift very far apart, even to an extent that eventually causes numerical breakdown at long integration times. In order to alleviate this issue, we converted the linear basis set parametrization to a parametrization based on polar decomposition, which allowed a (non-variational) restriction that was shown to enhance numerical stability by locking the bra and ket spaces together. The linear and polar parametrizations of Ref. 36 are exactly equivalent to the single exponential and double exponential parametrizations of the present work. In particular, the double exponential parametrization allows a restriction analogous to that of the restricted polar parametrization. We do not consider this restriction explicitly in the present work since it is easily introduced by setting appropriate matrix elements to zero (see Ref. 36 for details).

Returning to the derivations, we note that Eq. (48) implies that

$$e^{-\hat{\kappa}} \frac{de^{\hat{\kappa}}}{dt} = e^{-\hat{\kappa}'} e^{-\hat{\kappa}''} \frac{de^{\hat{\kappa}'} e^{\hat{\kappa}''}}{dt}, \quad (49)$$

which we will use as our starting point. Rather than rederiving everything from scratch, we will seek to convert the EOMs derived so far to the double exponential format. We start by

noting that the left-hand side of Eq. (49) can be written as

$$\begin{aligned}
e^{-\hat{\kappa}} \frac{de^{\hat{\kappa}}}{dt} &= \sum_{pq} \dot{\kappa}_{pq} e^{-\hat{\kappa}} \frac{\partial e^{\hat{\kappa}}}{\partial \kappa_{pq}} \\
&= \sum_{pq} \dot{\kappa}_{pq} D_{pq} \\
&= \sum_{pq} \sum_{rs} \dot{\kappa}_{pq} d_{(pq)(rs)} E_{rs} \\
&= -i \sum_{rs} g_{rs} E_{rs} \\
&= -i \hat{g}
\end{aligned} \tag{50}$$

where we have used Eqs. (15) and (24). The right-hand side is equal to

$$\begin{aligned}
e^{-\hat{\kappa}''} e^{-\hat{\kappa}'} \frac{de^{\hat{\kappa}'} e^{\hat{\kappa}''}}{dt} &= e^{-\hat{\kappa}''} \left(e^{-\hat{\kappa}'} \frac{de^{\hat{\kappa}'}}{dt} \right) e^{\hat{\kappa}''} + \left(e^{-\hat{\kappa}''} \frac{de^{\hat{\kappa}''}}{dt} \right) \\
&= e^{-\hat{\kappa}''} (-i \hat{g}') e^{\hat{\kappa}''} + (-i \hat{g}'')
\end{aligned} \tag{51}$$

with the definitions

$$\hat{g}' = i e^{-\hat{\kappa}'} \frac{de^{\hat{\kappa}'}}{dt}, \tag{52a}$$

$$\hat{g}'' = i e^{-\hat{\kappa}''} \frac{de^{\hat{\kappa}''}}{dt}. \tag{52b}$$

It follows from Eqs. (52) and the properties of $\hat{\kappa}'$ and $\hat{\kappa}''$ that

$$(\hat{g}')^\dagger = \hat{g}', \tag{53a}$$

$$(\hat{g}'')^\dagger = e^{\hat{\kappa}''} (-\hat{g}'') e^{-\hat{\kappa}''} \tag{53b}$$

which through Eqs. (48)–(51) implies

$$\hat{g} = e^{-\hat{\kappa}''} (\hat{g}' - (\hat{g}'')^\dagger) e^{\hat{\kappa}''}. \tag{54}$$

In matrix notation, this is

$$\begin{aligned}
\mathbf{G} &= e^{-\mathbf{K}''} (\mathbf{G}' - (\mathbf{G}'')^\dagger) e^{\mathbf{K}''} \\
&= \mathbf{P}^{-1} (\mathbf{G}' - (\mathbf{G}'')^\dagger) \mathbf{P}
\end{aligned} \tag{55}$$

where we have introduced $\mathbf{P} = e^{\mathbf{K}''}$ for notational convenience. Since we have taken the primitive basis to be orthonormal (see Sec. II B), the properties of the operators \hat{g}' and \hat{g}''

carry over directly to their matrix representations (we may for example conclude that the matrix \mathbf{G}' is Hermitian since the operator \hat{g}' is Hermitian). Equation (55) has exactly the same kind of structure that was encountered in Ref. 36. Similar to that work, we define a similarity transformed version of \mathbf{G} , i.e.

$$\bar{\mathbf{G}} = \mathbf{P}\mathbf{G}\mathbf{P}^{-1} = \mathbf{G}' - (\mathbf{G}'')^\dagger, \quad (56)$$

and use the Hermiticity of \mathbf{G}' to write

$$\mathbb{H}(\bar{\mathbf{G}}) = \mathbf{G}' - \mathbb{H}(\mathbf{G}''), \quad (57a)$$

$$\mathbb{A}(\bar{\mathbf{G}}) = \mathbb{A}(\mathbf{G}'') \quad (57b)$$

where \mathbb{H} and \mathbb{A} denote the Hermitian and anti-Hermitian parts, respectively, of a square matrix. In order to progress we combine $\mathbf{G}'' = \mathbb{A}(\mathbf{G}'') + \mathbb{H}(\mathbf{G}'')$ with the property from Eq. (53b) to get the following equation:

$$\mathbb{A}(\mathbf{G}'')\mathbf{P} - \mathbf{P}\mathbb{A}(\mathbf{G}'') = \mathbb{H}(\mathbf{G}'')\mathbf{P} + \mathbf{P}\mathbb{H}(\mathbf{G}''). \quad (58)$$

The matrix $\mathbf{P} = e^{\mathbf{K}''}$ is known from the outset while $\mathbb{A}(\mathbf{G}'')$ is given by Eq. (57b) and so the left-hand side of Eq. (58) is known. Equations such as Eq. (58) are called Lyapunov or, more generally, Sylvester equations and are well-known in the mathematical literature.⁴⁷ We showed in the appendix of Ref. 36 that Eq. (58) can be efficiently solved for $\mathbb{H}(\mathbf{G}'')$ provided that an eigenvalue decomposition of \mathbf{P} is available. Before stating the result, we diagonalize \mathbf{K}' (anti-Hermitian) and \mathbf{K}'' (Hermitian) as

$$\mathbf{K}' = \mathbf{S}\boldsymbol{\eta}\mathbf{S}^\dagger, \quad \mathbf{S}^\dagger\mathbf{S} = \mathbf{S}\mathbf{S}^\dagger = \mathbf{1}, \quad (59a)$$

$$\mathbf{K}'' = \mathbf{T}\boldsymbol{\zeta}\mathbf{T}^\dagger, \quad \mathbf{T}^\dagger\mathbf{T} = \mathbf{T}\mathbf{T}^\dagger = \mathbf{1}. \quad (59b)$$

The eigenvalues η_p are purely imaginary while the ζ_p are purely real. Equation (59b) allows us to write

$$\mathbf{P} = \exp(\mathbf{K}'') = \mathbf{T}\exp(\boldsymbol{\zeta})\mathbf{T}^\dagger = \mathbf{T}\boldsymbol{\epsilon}\mathbf{T}^\dagger \quad (60)$$

where the eigenvalues $\epsilon_p = \exp(\zeta_p)$, are purely real and strictly positive. The expression for $\mathbb{H}(\mathbf{G}'')$ now reads

$$\mathbb{H}(\mathbf{G}'') = \mathbf{T}(\boldsymbol{\Gamma} \circ (\mathbf{T}^\dagger \mathbb{A}(\bar{\mathbf{G}})\mathbf{T}))\mathbf{T}^\dagger \quad (61)$$

where the matrix $\mathbf{\Gamma}$ has elements

$$\gamma_{pq} = \frac{-\epsilon_p + \epsilon_q}{\epsilon_p + \epsilon_q}. \quad (62)$$

Note that $\mathbf{\Gamma}$ is real anti-symmetric and thus anti-Hermitian by construction. The denominator in Eq. (62) is always greater than zero since $\epsilon_p > 0$ as already mentioned. Combining Eqs. (57) and (61) now yields

$$\mathbf{G}' = \mathbb{H}(\bar{\mathbf{G}}) + \mathbf{T}(\mathbf{\Gamma} \circ (\mathbf{T}^\dagger \mathbb{A}(\bar{\mathbf{G}}) \mathbf{T})) \mathbf{T}^\dagger, \quad (63a)$$

$$\mathbf{G}'' = \mathbb{A}(\bar{\mathbf{G}}) + \mathbf{T}(\mathbf{\Gamma} \circ (\mathbf{T}^\dagger \mathbb{A}(\bar{\mathbf{G}}) \mathbf{T})) \mathbf{T}^\dagger. \quad (63b)$$

Having determined \mathbf{G}' and \mathbf{G}'' we recover $\dot{\mathbf{K}}'$ and $\dot{\mathbf{K}}''$ through transformations analogous to Eq. (47). For that purpose we construct the auxiliary matrices $\mathbf{\Omega}'$ and $\mathbf{\Omega}''$ with elements

$$\omega'_{pq} = 1/\varphi(\eta_p - \eta_q), \quad (64a)$$

$$\omega''_{pq} = 1/\varphi(\zeta_p - \zeta_q). \quad (64b)$$

The eigenvalues η_p and ζ_p are taken from Eqs. (59) and the function φ is given by Eq. (43). The resulting time derivatives then follow as

$$\dot{\mathbf{K}}' = -i\mathbf{S}(\mathbf{\Omega}' \circ (\mathbf{S}^\dagger \mathbf{G}' \mathbf{S})) \mathbf{S}^\dagger, \quad (65a)$$

$$\dot{\mathbf{K}}'' = -i\mathbf{T}(\mathbf{\Omega}'' \circ (\mathbf{T}^\dagger \mathbf{G}'' \mathbf{T})) \mathbf{T}^\dagger. \quad (65b)$$

The matrix \mathbf{K}'' has real eigenvalues and so the condition in Eq. (46) always holds. Thus Eq. (65b) is never singular. Conversely, the matrix \mathbf{K}' has purely imaginary eigenvalues so Eq. (65a) can become singular.

The overall procedure for the double exponential parametrization is as follows: (i) solve Eq. (25b) to obtain \mathbf{G} ; (ii) diagonalize \mathbf{K}' and \mathbf{K}'' as in Eqs. (59); (iii) compute $\bar{\mathbf{G}}$ in Eq. (56); (iv) compute \mathbf{G}' and \mathbf{G}'' in Eqs. (63); and (v) recover $\dot{\mathbf{K}}'$ and $\dot{\mathbf{K}}''$ from Eqs. (65). The discussion of computational cost is completely analogous to that at the end of Sec. II E.

G. Removing singularities

Before implementing the single and double exponential basis set EOMs, we need to address the possible singularities. We first note that one is not likely to encounter exact singularities in a numerical settings but rather near-singularities. Such near-singularities will not necessarily

cause numerical breakdown but they will result in very large $\dot{\mathbf{K}}^m$ (single exponential case) or $\dot{\mathbf{K}}'^m$ (double exponential case), thus making the EOMs hard to propagate. We expect that a good, adaptive integrator will be able to manage such difficulties at the price of temporarily reducing the step size. Although such a situation is not disastrous it should be avoided since the cost of propagating the wave function is inversely proportional to the average step size.

For the single exponential case, we remove a (near-)singularity in a given mode m by absorbing the non-zero $\hat{\kappa}^m$ into the Hamiltonian:

$$H \leftarrow \exp(-\hat{\kappa}^m) H \exp(\hat{\kappa}^m) \quad (66)$$

In practice this simply amounts to transforming the Hamiltonian integrals and resetting $\hat{\kappa}^m$ to zero (equivalently, this process can be phrased as a transformation of the primitive basis). The same procedure applies to $\hat{\kappa}'^m$ in the double exponential case and we note that a transformation by the unitary operator $\exp(\hat{\kappa}'^m)$ keeps the primitive basis orthonormal (which was needed for the derivations in Sec. [II F](#)).

As a criterion for resetting mode m , we take the simple approach of monitoring the numbers $\varphi_{p^m q^m}^m = \varphi(\mu_{p^m}^m - \mu_{q^m}^m)$, which in the single exponential case are simply the eigenvalues of $(\mathbf{D}^m)^\top$; see Eqs. [\(43\)](#) and [\(46\)](#). We currently perform the reset of mode m if

$$|\varphi_{\min}^m| = \min_{p^m q^m} |\varphi_{p^m q^m}^m| < \tau \quad (67)$$

where τ is a user-defined threshold. The minimum eigenvalue has the benefit of not scaling significantly with the size of the primitive basis in contrast to e.g. the determinant of $(\mathbf{D}^m)^\top$ (which is the product of the eigenvalues).

It should be noted that algorithms for integrating ordinary differential equations (ODEs) typically evaluate the EOMs several times in order to determine an appropriate step. We perform the check in Eq. [\(67\)](#) after each such evaluation but the reset is only done after the step is completed and if the criterion was fulfilled at least once. Choosing the threshold τ sufficiently large results in the reset of every mode after every integrator step.

H. Comparison to local derivatives

Section II G describes how one can reset non-zero $\hat{\kappa}^m$ in order to avoid (near-)singularities in the EOMs. Having $\hat{\kappa}^m = 0$ also results in simpler working equations, e.g.

$$\dot{\mathbf{K}}^m = -i\mathbf{G}^m, \quad (68)$$

and one could thus consider an approach where the resets are performed before every evaluation of the EOMs, thus basing the propagation on temporally local derivatives of the Lagrangian. This is indeed the approach taken by Kristiansen et al.³⁴ in their derivation of (electronic) time-dependent orbital-optimized coupled cluster with double excitations (TDOCCD), non-orthogonal TDOCCD (TDNOCCD) and the corresponding second-order approximations TDOMP2 and TDNOMP2.

Although formally equivalent, it is not immediately clear to us that the two approaches are fully equivalent in a numerical setting where time is discretized. To illustrate the point, consider the situation where initially $\hat{\kappa}^m = 0$ for each mode. For the two sets of EOMs to be completely equivalent, we require that they result in the same integrator step, i.e. they should describe the same physical evolution of the system. For definiteness, we consider a general (explicit or implicit) Runge-Kutta method^{48,49}:

$$\mathbf{y}_{n+1} = \mathbf{y}_n + h \sum_{i=1}^s b_i \mathbf{k}_i \quad (69a)$$

$$\mathbf{k}_i = f(t_n + c_i h, \mathbf{y}_n + h \sum_{j=1}^s a_{ij} \mathbf{k}_j), \quad i = 1, \dots, s \quad (69b)$$

Here, \mathbf{y}_n and \mathbf{y}_{n+1} are the vectors containing current and updated parameters, h is the step size, the scalars c_i , b_i and a_{ij} are the parameters defining the method, s is the number of stages and $f(t, \mathbf{y}) = \dot{\mathbf{y}}(t, \mathbf{y})$. The auxiliary vectors \mathbf{k}_i should satisfy the (generally non-linear) equations in Eq. (69b). Since the two approaches result in numerically different values of $f(t, \mathbf{y})$, it seems to us that the solution to Eq. (69b) and thus the integrator step predicted by Eq. (69a) will differ (also when the $\hat{\kappa}^m$ are initially equal to zero). We hypothesize that this difference is small when h is small. Thus, this work does not question the usefulness of the local derivative approach. Rather, the point is that while the general formulation for non-zero $\hat{\kappa}^m$ might seem very complicated at the outset, it turns out that it is in fact simple to implement with limited computational cost as discussed in Sec. II E.

III. IMPLEMENTATION

The single and double exponential modal EOMs have been implemented in the Molecular Interactions, Dynamics and Simulations Chemistry Program Package (MidasCpp)⁵⁰ in conjunction with the TDMVCC³⁵ method. The existing TDMVCC code has been refactored to make it largely agnostic to the parametrization of the modals. Modal parameters are now stored in an abstract class that is easily specialized using C++ class inheritance. We note that the computationally intensive parts of the code are independent of the choice of modal parametrization.

This modular design is possible since the time evolution of the modals is always governed by the same set of equations, Eq. (25b). Having solved these equations (which is a major computational task), the additional steps leading to linear³⁵, polar³⁶ or exponential parametrization (this work) are all simple and cheap to perform. The computational overhead resulting from the exponential parametrization (which requires the diagonalization of one-mode quantities and a number of one-mode transformations) scales linearly with respect to the number of modes and is negligible for all but the smallest systems.

We note that the TDMVCC method is presently implemented using the general but inefficient full-space matrix representation (FSMR) framework that was introduced in Ref. 45. This limits our calculations to small systems (approximately six modes and rather small active basis sets). Efficient, polynomial-scaling implementations of TDMVCC are the subject of current research in our group.

IV. NUMERICAL EXAMPLES

A. Computational details

We consider two numerical examples from Ref. 35 in order to study the performance and stability of the single and double exponential modal parametrizations. The first example is the intramolecular vibrational energy redistribution (IVR) of water after the excitation of the symmetric stretch to $n = 2$. The initial state is obtained as the $[0, 2, 0]$ state on the harmonic part of the potential energy surface (PES), i.e. the initial state is a simple harmonic oscillator state. The wave packet is then propagated at the TDMVCC[2] level on the full (anharmonic and coupled) PES using the Dormand-Prince 8(5,3) (DOP853) integrator⁴⁸ with

integrator tolerances $\tau_{\text{abs}} = 10^{-10}$ and $\tau_{\text{rel}} = 10^{-10}$. The calculation uses 30 primitive modals and 4 active modals for each mode.

The second example is the Franck–Condon emission ($S_1 \rightarrow S_0$) of the 5D *trans*-bithiophene model of Ref. 51. The initial state is taken to be the VSCF ground state of the S_1 electronic surface. The wave packet is then placed on the S_0 surface and propagated at the TDMVCC[2] level using the same integrator settings as above. Once again, we use 30 primitive and 4 active modals for each mode.

For both examples we repeat the calculations using linearly parametrized modals (see Refs. 35 and 36) and with single and double exponentially parametrized modals. Reset thresholds $\tau = 0, 0.1, 0.3, 0.5, 0.7, \infty$ are considered. The threshold $\tau = 0$ corresponds to never resetting the basis set parameters, while the threshold $\tau = \infty$ corresponds to resetting after every step.

In both cases we show autocorrelation functions (ACFs) to illustrate the equivalence of the various modal parametrizations. The ACF is not an observable as such but conveys important information about the dynamics of the system while being sensitive to errors in the wave function parameters.

B. Autocorrelation functions

Figure 1 shows ACFs for the linear and single exponential water IVR calculations. The ACFs all coincide perfectly, demonstrating the numerical equivalence of the various modal parametrizations. The dynamics is strongly oscillatory with a dominating period of roughly 370 a.u. (9 fs).

Figure 2 display ACFs for the 5D *trans*-bithiophene model using linearly and double exponentially parametrized modals. We once again observe perfect agreement between the different parametrizations. This time the dynamics is significantly slower, which is also reflected in the integrator step size (see later).

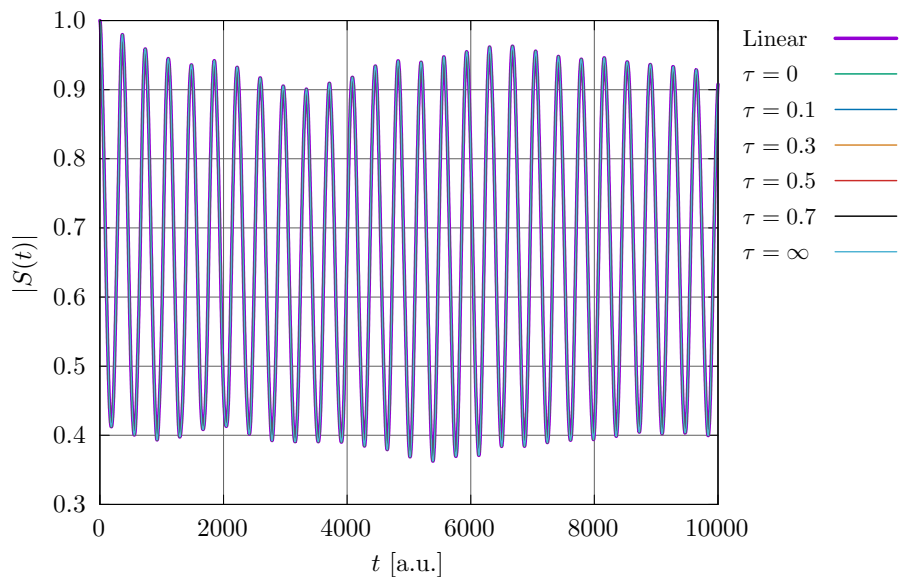


Figure 1. ACFs for the IVR of water described at the TDMVCC[2] level. The reference calculation (purple) uses linearly parametrized modals, while the remaining calculations use single exponentially parametrized modals with a number of reset thresholds τ (see text). Note that the lines coincide so some are not visible.

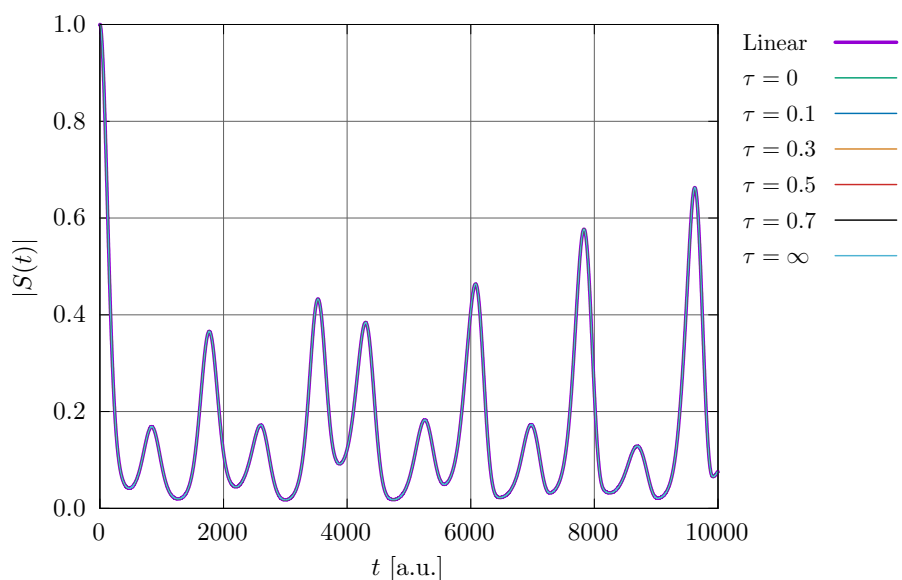


Figure 2. ACFs for the 5D *trans*-bithiophene model described at the TDMVCC[2]. The reference calculation (purple) uses linearly parametrized modals, while the remaining calculations use double exponentially parametrized modals with a number of reset thresholds τ (see text). Note that the lines coincide so some are not visible.

C. Integrator step size

Having demonstrated the equivalence of the linear and exponential formalisms (and the correctness of the implementation) we turn to examine their performance and behaviour with respect to the integrator step size. Figure 3 shows the step size and the minimum eigenvalues $|\varphi_{\min}^m|$ of Eq. (67) for the water IVR calculation using single exponentially parametrized modals and $\tau = 0$ (i.e. no resets). The step size exhibits a series of very sharp dips that coincide with small values of $|\varphi_{\min}^m|$. This is exactly the kind of near-singularity behaviour that was described in Sec. II G. In this particular case, it seems that mode 1 (i.e. the symmetric stretch, which was initially excited) is responsible for most near-singularities in the time interval shown. We note that the near-singularities are very short-lived and that the integrator is perfectly capable of stepping through them. This suggests that the formal existence of singularities in the modal EOMs is not catastrophic in a numerical setting. In Fig. 4, the water IVR calculation is repeated with $\tau = 0.1$. The resets are clearly visible in the figure and have the effect of removing any (near-)singularities. As a consequence, the step size is stabilized close to its mean value.

Analogous results are shown for the 5D *trans*-bithiophene model in Figs. 5 and 6 (using double exponentially parametrized modals). A few near-singularities are also observed for this system but they are much less frequent compared to the water IVR case (this difference can be explained partially by the fact that the *trans*-bithiophene dynamics is simply slower). The near-singularities are again removed efficiently by the threshold-based resets.

Figures S1–S4 in the supplementary material show very similar behaviour for the IVR of water with double exponential modals and the 5D *trans*-bithiophene model with single exponential modals.

In order to assess performance in a more quantitative fashion we present average step sizes (h_{mean}) for water and *trans*-bithiophene in Tables I and II. The tables also include the mean stepsize relative to a reference calculation with linearly parametrized modals, i.e.

$$h_{\text{rel}} = \frac{h_{\text{mean}}}{h_{\text{mean}}^{\text{linear}}}. \tag{70}$$

For water (Table I), the thresholds $\tau = 0$ (no resets) and $\tau = \infty$ (reset after every step) perform slightly worse than the linear reference for single as well as double exponential calculations. Considering Fig. 3, it is perhaps not surprising that $\tau = 0$ leads to smaller

average steps due to the near-singularities. The remaining thresholds ($\tau = 0.1, 0.3, 0.5, 0.7$) all perform slightly better than the linear reference, although the difference is small (on the order of a few percent). The single and double exponential calculations perform essentially the same.

For *trans*-bithiophene (Table II), all calculations with exponentially parametrized modals perform slightly better than the reference except for the single exponential calculation with $\tau = 0$. The double exponentially parametrized modals result in slightly larger average steps compared to the single exponential case, but the difference is again small.

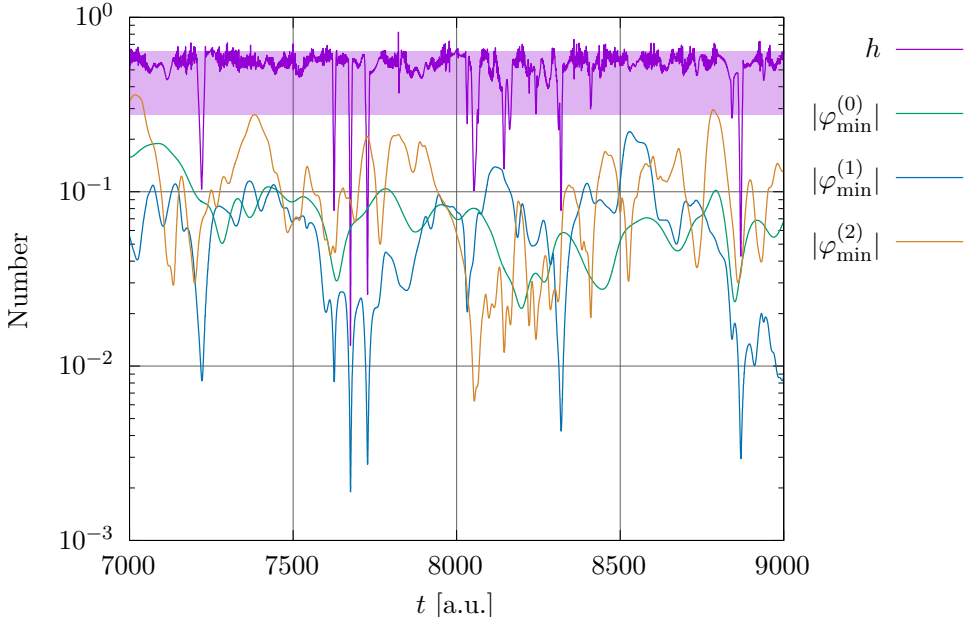


Figure 3. Integrator step size (h) and $|\varphi_{\min}^m|$ for the IVR of water described at the TDMVCC[2] level using single exponentially parametrized modals ($\tau = 0$, i.e. no resets). The shaded area covers the mean step size plus/minus its standard deviation (computed within the shown time interval). Only part of the full time interval is shown for greater visibility.

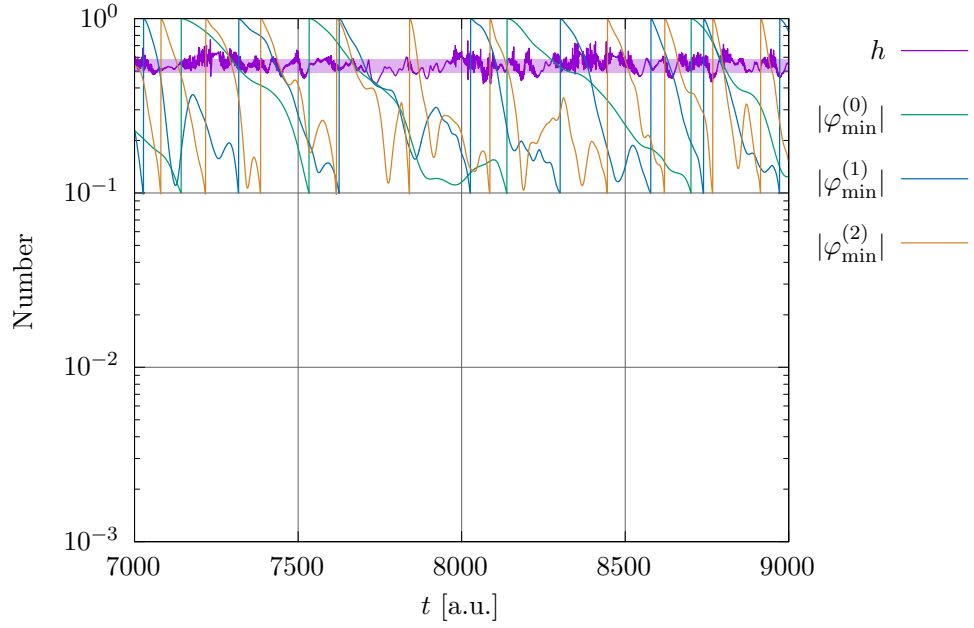


Figure 4. Integrator step size (h) and $|\varphi_{\min}^m|$ for the IVR of water described at the TDMVCC[2] level using single exponentially parametrized modals ($\tau = 0.1$). The shaded area covers the mean step size plus/minus its standard deviation (computed within the shown time interval). Only part of the full time interval is shown for greater visibility.

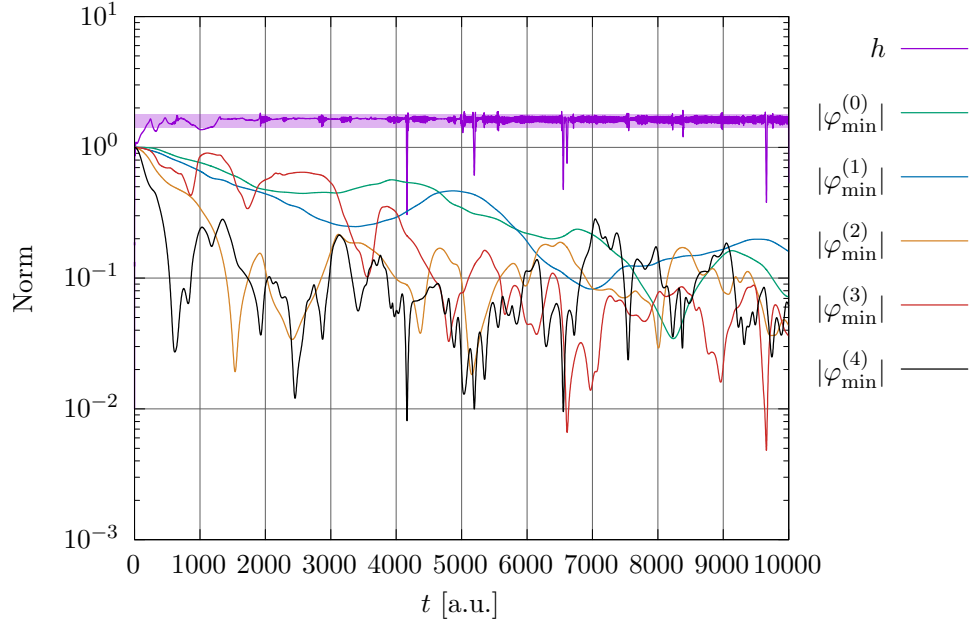


Figure 5. Integrator step size (h) and $|\varphi_{\min}^m|$ for the 5D *trans*-bithiophene model described at the TDMVCC[2] level using double exponentially parametrized modals ($\tau = 0$, i.e. no resets). The shaded area covers the mean step size plus/minus its standard deviation.

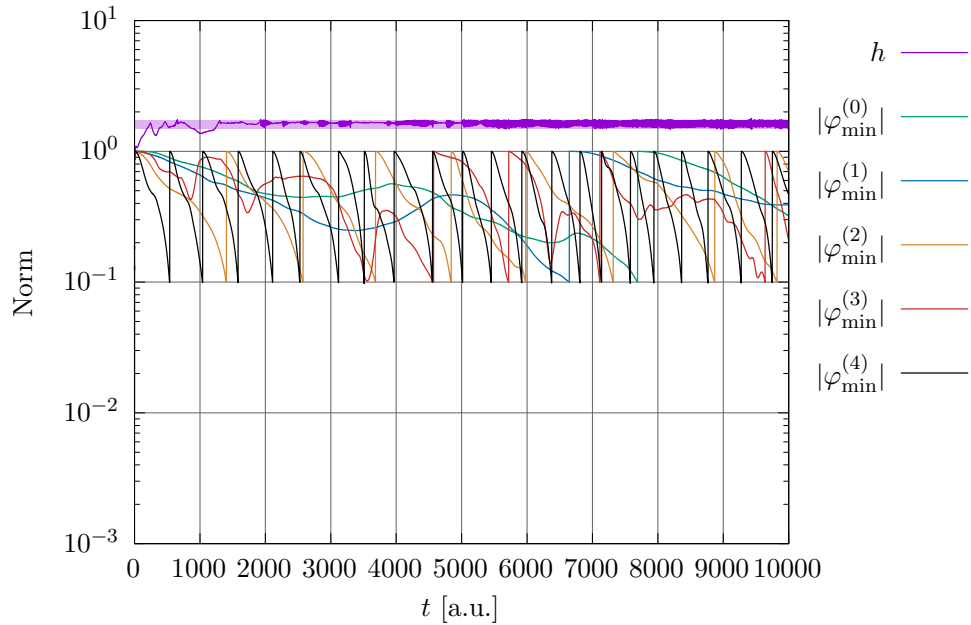


Figure 6. Integrator step size (h) and $|\varphi_{\min}^m|$ for the 5D *trans*-bithiophene model described at the TDMVCC[2] level using double exponentially parametrized modals ($\tau = 0.1$). The shaded area covers the mean step size plus/minus its standard deviation.

Table I. Mean and relative step sizes for the IVR of water described at the TDMVCC[2] level. h_{mean} is given in atomic units and h_{rel} is given relative to the linear case.

Type	τ	h_{mean}	h_{rel}
Linear	—	0.4088	1.0000
Single	0	0.3880	0.9491
	0.1	0.4182	1.0229
	0.3	0.4175	1.0211
	0.5	0.4151	1.0154
	0.7	0.4119	1.0075
	∞	0.4080	0.9979
	Double	0	0.3879
0.1		0.4178	1.0220
0.3		0.4174	1.0210
0.5		0.4151	1.0154
0.7		0.4129	1.0099
∞		0.4079	0.9977

Table II. Mean and relative step sizes for the 5D *trans*-bithiophene model described at the TDMVCC[2] level. h_{mean} is given in atomic units and h_{rel} is given relative to the linear case.

Type	τ	h_{mean}	h_{rel}
Linear	—	1.5704	1.0000
Single	0	1.5574	0.9917
	0.1	1.6075	1.0236
	0.3	1.6080	1.0240
	0.5	1.6088	1.0245
	0.7	1.6090	1.0246
	∞	1.6100	1.0253
Double	0	1.5901	1.0126
	0.1	1.6184	1.0306
	0.3	1.6186	1.0308
	0.5	1.6194	1.0313
	0.7	1.6184	1.0306
	∞	1.6202	1.0318

V. SUMMARY AND OUTLOOK

A general set of EOMs for time-dependent wave functions with exponentially parametrized biorthogonal basis sets has been derived in a fully bivariational framework. The non-trivial connection to the EOMs for linearly parametrized basis sets was elucidated, thus offering a unified perspective on the two approaches. In particular, it was shown that the computationally intensive parts are in fact identical for the two kinds of parametrizations. The exponential parametrization can thus be implemented on top of existing code with limited programming effort.

Careful analysis of the equations showed the existence of a well-defined set of singularities related to the eigenvalues of the matrices containing the basis set parameters. It was demonstrated how these singularities can be removed in a controlled manner by a simple

update of the Hamiltonian integrals. The monitoring of singularities requires only quantities that are computed in any case.

The exponential EOMs were subsequently used as a starting point for deriving EOMs for a double exponential parametrization, thus providing a separation of the basis set time evolution into a unitary part and a part describing the deviation from unitarity. The transformations necessary to obtain the double exponential formulation again carry negligible additional cost.

Finally, we presented numerical results for calculations on water and a 5D *trans*-bithiophene model. The calculations showed that the single and double exponential parametrizations result in slightly larger step sizes compared to linearly parametrized reference calculations. Although the effect on step size is minor, our findings underline the fact that one should not necessarily consider the exponential basis set parametrization as more costly compared to the linear parametrization. We have argued that the additional operations needed for the exponential parametrization are computationally cheap, while an increase in the average integrator step size leads directly to fewer costly evaluations of the EOMs.

Although the present work focuses on bivariational wave functions, we note that the mathematical machinery for converting between linearly and exponentially parametrized basis sets is also applicable to other types of wave functions. We thus anticipate that these results will be useful in future treatments of both nuclear quantum dynamics and time-dependent electronic structure.

SUPPLEMENTARY MATERIAL

The supplementary material contains additional figures related to the water and 5D *trans*-bithiophene calculations presented within the article.

ACKNOWLEDGEMENTS

O.C. acknowledges support from the Independent Research Fund Denmark through grant number 1026-00122B. Computations were performed at the Centre for Scientific Computing Aarhus (CSCAA).

AUTHOR DECLARATIONS

Conflict of Interest

The authors have no conflicts to disclose.

Author Contributions

Mads Greisen Højlund: Conceptualization (equal); Data curation (lead); Formal analysis (equal); Investigation (lead); Software (lead); Visualization (lead); Writing – original draft (lead); Writing – review & editing (equal). **Alberto Zoccante:** Conceptualization (equal); Formal analysis (equal); Writing – review & editing (equal). **Ove Christiansen:** Conceptualization (equal); Formal analysis (equal); Funding acquisition (lead); Project administration (lead); Supervision (lead); Writing – review & editing (equal).

DATA AVAILABILITY

The data that supports the findings of this study are available within the article and its supplementary material.

Appendix A: Similarity transformed derivative: Specialization

Direct application of Eq. (41) shows that

$$D_{pq} = e^{-\hat{\kappa}} \frac{\partial e^{\hat{\kappa}}}{\partial \kappa_{pq}} = \sum_{rs} d_{(pq)(rs)} E_{rs} \quad (\text{A1})$$

where we have reintroduced explicit summation and left out the mode index m to avoid notational clutter. This is identical to Eq. (15) but now includes a concrete recipe for computing the \mathbf{D} matrix. In order to actually carry out the computation we need to consider the structure constants describing the generators E_{pq} . By writing

$$[E_{pq}, E_{rs}] = \delta_{qr} E_{ps} - \delta_{ps} E_{rq} \quad (\text{A2})$$

$$= \sum_{\bar{r}\bar{s}} (\delta_{qr} \delta_{\bar{r}p} \delta_{\bar{s}s} - \delta_{ps} \delta_{\bar{r}r} \delta_{\bar{s}q}) E_{\bar{r}\bar{s}} \quad (\text{A3})$$

we see that

$$f_{(pq)(rs)}^{\bar{r}\bar{s}} = (\delta_{qr}\delta_{\bar{r}p}\delta_{\bar{s}s} - \delta_{ps}\delta_{\bar{r}r}\delta_{\bar{s}q}). \quad (\text{A4})$$

The \mathbf{Q} matrix is now given by

$$\begin{aligned} Q_{(rs)(\bar{r}\bar{s})} &= \sum_{pq} \kappa_{pq} f_{(pq)(rs)}^{\bar{r}\bar{s}} \\ &= \sum_{pq} \kappa_{pq} \delta_{qr} \delta_{\bar{r}p} \delta_{\bar{s}s} - \sum_{pq} \kappa_{pq} \delta_{ps} \delta_{\bar{r}r} \delta_{\bar{s}q} \\ &= \kappa_{\bar{r}r} \delta_{\bar{s}s} - \kappa_{s\bar{s}} \delta_{\bar{r}r} \end{aligned} \quad (\text{A5})$$

or, equivalently,

$$\begin{aligned} \mathbf{Q} &= \mathbf{K}^T \otimes \mathbf{1} - \mathbf{1} \otimes \mathbf{K} \\ &= \mathbf{K}^T \otimes \mathbf{1} + \mathbf{1} \otimes (-\mathbf{K}) \\ &= \mathbf{K}^T \oplus (-\mathbf{K}). \end{aligned} \quad (\text{A6})$$

Here, \otimes denotes the Kronecker product while \oplus denotes the so-called Kronecker sum. The simple structure in Eq. (A6) allows us to analyse and manipulate the \mathbf{Q} matrix in a convenient way. Let \mathbf{K} have eigenvalues μ_1, \dots, μ_N where N is the order of the matrix. Then $-\mathbf{K}$ has eigenvalues $-\mu_1, \dots, -\mu_N$ while \mathbf{Q} has eigenvalues⁴⁷

$$\lambda_{pq} = \mu_p - \mu_q, \quad p, q = 1, \dots, N. \quad (\text{A7})$$

We see that \mathbf{Q} has at least N eigenvalues equal to zero and so \mathbf{Q} is always singular. Now assume that \mathbf{K} is diagonalizable as

$$\mathbf{K} = \mathbf{R}\boldsymbol{\mu}\mathbf{L}^\dagger, \quad \mathbf{L}^\dagger\mathbf{R} = \mathbf{R}\mathbf{L}^\dagger = \mathbf{1} \quad (\text{A8})$$

where $\boldsymbol{\mu}$ is a diagonal matrix holding the eigenvalues μ_p . In the notation of Eq. (A8), the rows of \mathbf{L}^\dagger are the left eigenvectors of \mathbf{K} while the columns of \mathbf{V} are the right eigenvectors of \mathbf{K} . In addition, let

$$\boldsymbol{\Lambda} = \boldsymbol{\mu} \otimes \mathbf{1} - \mathbf{1} \otimes \boldsymbol{\mu} \quad (\text{A9})$$

be the diagonal matrix holding the eigenvalues $\lambda_{pq} = \mu_p - \mu_q$ of \mathbf{Q} . It follows directly that

$$\begin{aligned} (\mathbf{L}^* \otimes \mathbf{R})\boldsymbol{\Lambda}(\mathbf{R}^T \otimes \mathbf{L}^\dagger) &= (\mathbf{L}^* \otimes \mathbf{R})(\boldsymbol{\mu} \otimes \mathbf{1} - \mathbf{1} \otimes \boldsymbol{\mu})(\mathbf{R}^T \otimes \mathbf{L}^\dagger) \\ &= (\mathbf{L}^* \boldsymbol{\mu} \mathbf{R}^T) \otimes (\mathbf{R} \mathbf{L}^\dagger) - (\mathbf{L}^* \mathbf{R}^T) \otimes (\mathbf{R} \boldsymbol{\mu} \mathbf{L}^\dagger) \\ &= \mathbf{K}^T \otimes \mathbf{1} - \mathbf{1} \otimes \mathbf{K} \\ &= \mathbf{Q}. \end{aligned} \quad (\text{A10})$$

We see that \mathbf{Q} can be diagonalized in a simple way provided \mathbf{K} is diagonalizable. The matrices

$$\mathfrak{R} = \mathbf{L}^* \otimes \mathbf{R} \quad (\text{A11a})$$

$$\mathfrak{L}^\dagger = \mathbf{R}^\top \otimes \mathbf{L}^\dagger \quad (\text{A11b})$$

contain the right and left eigenvectors of \mathbf{Q} , respectively, and satisfy $\mathfrak{L}^\dagger \mathfrak{R} = \mathfrak{R} \mathfrak{L}^\dagger = \mathbf{1}$ due to Eq. (A8). Following Eq. (42), we are now ready to compute

$$\mathbf{D} = \mathfrak{R} \varphi(\Lambda) \mathfrak{L}^\dagger = \mathfrak{R} \Phi \mathfrak{L}^\dagger, \quad (\text{A12a})$$

$$\mathbf{D}^\top = \mathfrak{L}^* \varphi(\Lambda) \mathfrak{R}^\top = \mathfrak{L}^* \Phi \mathfrak{R}^\top \quad (\text{A12b})$$

where the diagonal matrix Φ has diagonal elements

$$\varphi_{pq} = \varphi(\lambda_{pq}) = \varphi(\mu_p - \mu_q). \quad (\text{A13})$$

If \mathbf{D} and thus \mathbf{D}^\top is invertible, we write

$$\mathbf{D}^{-\top} = \mathfrak{L}^* \Phi^{-1} \mathfrak{R}^\top \quad (\text{A14})$$

and proceed to compute the matrix-vector product

$$\begin{aligned} \dot{\boldsymbol{\kappa}} &= -i \mathbf{D}^{-\top} \mathbf{g} \\ &= -i \mathfrak{L}^* \Phi^{-1} \mathfrak{R}^\top \mathbf{g} \\ &= -i (\mathbf{R} \otimes \mathbf{L}^*) \Phi^{-1} (\mathbf{L}^\dagger \otimes \mathbf{R}^\top) \mathbf{g}. \end{aligned} \quad (\text{A15})$$

This exact type of product was encountered in the appendix of Ref. 36 and can be simplified by using that

$$(\mathbf{A} \otimes \mathbf{B}) \text{vec}(\mathbf{C}) = \text{vec}(\mathbf{A} \mathbf{C} \mathbf{B}^\top) \quad (\text{A16})$$

where $\text{vec}(\cdot)$ denotes the row-major vectorization mapping. Rather than repeating the steps, we simply state the result:

$$\dot{\mathbf{K}} = -i \mathbf{R} (\Omega \circ (\mathbf{L}^\dagger \mathbf{G} \mathbf{R})) \mathbf{L}^\dagger. \quad (\text{A17})$$

Here, $\dot{\mathbf{K}}$ and \mathbf{G} are the matrices holding the elements of the vectors $\dot{\boldsymbol{\kappa}}$ and \mathbf{g} , respectively, while the symbol \circ denotes the Hadamard (or element-wise) product. We have, in addition,

introduced the $N \times N$ matrix $\mathbf{\Omega}$ that holds the N^2 diagonal elements of the $N^2 \times N^2$ diagonal matrix $\mathbf{\Phi}^{-1}$, i.e.

$$\omega_{pq} = 1/\varphi(\lambda_{pq}) = 1/\varphi(\mu_p - \mu_q). \quad (\text{A18})$$

This result holds, as mentioned, when \mathbf{D}^\top is invertible. According to the discussion in Sec. IID, this is the case exactly when

$$\mu_p - \mu_q \neq 2\pi ik \quad (\text{A19})$$

where k is a non-zero integer.

REFERENCES

- ¹D. Zgid and M. Nooijen, *J. Chem. Phys.* **128**, 144116 (2008).
- ²D. Ghosh, J. Hachmann, T. Yanai, and G. K.-L. Chan, *J. Chem. Phys.* **128**, 144117 (2008).
- ³Y. Ma, S. Knecht, S. Keller, and M. Reiher, *J. Chem. Theory Comput.* **13**, 2533 (2017).
- ⁴C. D. Sherrill, A. I. Krylov, E. F. C. Byrd, and M. Head-Gordon, *J. Chem. Phys.* **109**, 4171 (1998).
- ⁵T. B. Pedersen, H. Koch, and C. Hättig, *J. Chem. Phys.* **110**, 8318 (1999).
- ⁶T. B. Pedersen, B. Fernández, and H. Koch, *J. Chem. Phys.* **114**, 6983 (2001).
- ⁷J. Arponen, *Ann. Phys.* **151**, 311 (1983).
- ⁸R. H. Myhre, *J. Chem. Phys.* **148**, 094110 (2018).
- ⁹A. Köhn and J. Olsen, *J. Chem. Phys.* **122**, 084116 (2005).
- ¹⁰H.-D. Meyer, U. Manthe, and L. Cederbaum, *Chem. Phys. Lett.* **165**, 73 (1990).
- ¹¹M. H. Beck, A. Jäckle, G. A. Worth, and H.-D. Meyer, *Phys. Rep.* **324**, 1 (2000).
- ¹²J. Zanghellini, M. Kitzler-Zeiler, C. Fabian, T. Brabec, and A. Scrinzi, *Laser Phys.* **13**, 1064 (2003).
- ¹³J. Caillat, J. Zanghellini, M. Kitzler, O. Koch, W. Kreuzer, and A. Scrinzi, *Phys. Rev. A* **71**, 012712 (2005).
- ¹⁴T. Kato and H. Kono, *Chem. Phys. Lett.* **392**, 533 (2004).
- ¹⁵T. Sato and K. L. Ishikawa, *Phys. Rev. A* **88**, 023402 (2013).
- ¹⁶H. Miyagi and L. B. Madsen, *Phys. Rev. A* **87**, 062511 (2013).
- ¹⁷D. J. Haxton and C. W. McCurdy, *Phys. Rev. A* **91**, 012509 (2015).
- ¹⁸T. Sato and K. L. Ishikawa, *Phys. Rev. A* **91**, 023417 (2015).
- ¹⁹G. A. Worth, *J. Chem. Phys.* **112**, 8322 (2000).
- ²⁰R. Wodraszka and T. Carrington, *J. Chem. Phys.* **145**, 044110 (2016).
- ²¹H. R. Larsson and D. J. Tannor, *J. Chem. Phys.* **147**, 044103 (2017).
- ²²N. K. Madsen, M. B. Hansen, G. A. Worth, and O. Christiansen, *J. Chem. Phys.* **152**, 084101 (2020).
- ²³N. K. Madsen, M. B. Hansen, G. A. Worth, and O. Christiansen, *J. Chem. Theory Comput.* **16**, 4087 (2020).
- ²⁴O. E. Alon, A. I. Streltsov, and L. S. Cederbaum, *Phys. Rev. A* **76**, 062501 (2007).
- ²⁵O. E. Alon, A. I. Streltsov, and L. S. Cederbaum, *Phys. Rev. A* **77**, 033613 (2008).

- ²⁶M. Nest, *Chemical Physics Letters* **472**, 171 (2009).
- ²⁷U. Manthe and T. Weike, *J. Chem. Phys.* **146**, 064117 (2017).
- ²⁸S. Kvaal, *J. Chem. Phys.* **136**, 194109 (2012).
- ²⁹T. Sato, H. Pathak, Y. Orimo, and K. L. Ishikawa, *J. Chem. Phys.* **148**, 051101 (2018).
- ³⁰T. B. Pedersen and S. Kvaal, *J. Chem. Phys.* **150**, 144106 (2019).
- ³¹H. E. Kristiansen, Ø. S. Schøyen, S. Kvaal, and T. B. Pedersen, *J. Chem. Phys.* **152**, 071102 (2020).
- ³²H. Pathak, T. Sato, and K. L. Ishikawa, *J. Chem. Phys.* **153**, 034110 (2020).
- ³³H. Pathak, T. Sato, and K. L. Ishikawa, *J. Chem. Phys.* **154**, 234104 (2021).
- ³⁴H. E. Kristiansen, B. S. Ofstad, E. Hauge, E. Aurbakken, Ø. S. Schøyen, S. Kvaal, and T. B. Pedersen, *J. Chem. Theory Comput.* **18**, 3687 (2022).
- ³⁵N. K. Madsen, M. B. Hansen, O. Christiansen, and A. Zocante, *J. Chem. Phys.* **153**, 174108 (2020).
- ³⁶M. G. Højlund, A. B. Jensen, A. Zocante, and O. Christiansen, *J. Chem. Phys.* **157**, 234104 (2022).
- ³⁷T. Helgaker, P. Jørgensen, and J. Olsen, *Molecular Electronic-Structure Theory* (Wiley, Chichester ; New York, 2000).
- ³⁸T. B. Pedersen and H. Koch, *J. Chem. Phys.* **108**, 12 (1998).
- ³⁹N. K. Madsen, M. B. Hansen, A. Zocante, K. Monrad, M. B. Hansen, and O. Christiansen, *J. Chem. Phys.* **149**, 134110 (2018).
- ⁴⁰P. Kramer and M. Saraceno, *Geometry of the Time-Dependent Variational Principle in Quantum Mechanics*, Lecture Notes in Physics, Vol. 140 (Springer Berlin Heidelberg, Berlin, Heidelberg, 1981).
- ⁴¹K. Ohta, *Phys. Rev. A* **70**, 022503 (2004).
- ⁴²O. Christiansen, *J. Chem. Phys.* **120**, 2140 (2004).
- ⁴³B. C. Hall, *Lie Groups, Lie Algebras, and Representations*, Graduate Texts in Mathematics, Vol. 222 (Springer International Publishing, Cham, 2015).
- ⁴⁴J. Olsen and P. Jørgensen, *J. Chem. Phys.* **82**, 3235 (1985).
- ⁴⁵M. B. Hansen, N. K. Madsen, and O. Christiansen, *J. Chem. Phys.* **153**, 044133 (2020).
- ⁴⁶J. Olsen, *J. Chem. Phys.* **143**, 114102 (2015).
- ⁴⁷A. J. Laub, *Matrix Analysis for Scientists and Engineers* (Society for Industrial and Applied Mathematics, Philadelphia, 2005).

- ⁴⁸E. Hairer, S. P. Nørsett, and G. Wanner, *Solving Ordinary Differential Equations I: Nonstiff Problems*, 2nd ed., Springer Series in Computational Mathematics No. 8 (Springer, Heidelberg ; London, 2009).
- ⁴⁹E. Hairer, C. Lubich, and G. Wanner, *Geometric Numerical Integration: Structure-Preserving Algorithms for Ordinary Differential Equations*, 2nd ed., Springer Series in Computational Mathematics No. 31 (Springer, Berlin ; New York, 2006).
- ⁵⁰D. G. Artiukhin, O. Christiansen, I. H. Godtlielsen, E. M. Gras, W. Györfy, M. B. Hansen, M. B. Hansen, E. L. Klinting, J. Kongsted, C. König, D. Madsen, N. K. Madsen, K. Monrad, G. Schmitz, P. Seidler, K. Sneskov, M. Sparta, B. Thomsen, D. Toffoli, A. Zoccante, M. G. Højlund, N. M. Høyer, and A. B. Jensen, “MidasCpp,” (2022).
- ⁵¹D. Madsen, O. Christiansen, P. Norman, and C. König, *Phys. Chem. Chem. Phys.* **21**, 17410 (2019).

General exponential basis set parametrization: Application to time-dependent bivariational wave functions: Supplementary material

Mads Greisen Højlund,^{1, a)} Alberto Zocante,^{2, b)} and Ove Christiansen^{1, c)}

¹⁾*Department of Chemistry, University of Aarhus,
Langelandsgade 140, DK-8000 Aarhus C, Denmark*

²⁾*Dipartimento di Scienze e Innovazione Tecnologica, Università del Piemonte
Orientale (UPO), Via T. Michel 11, 15100 Alessandria, Italy*

(Dated: March 30, 2023)

^{a)}Electronic mail: madsgh@chem.au.dk

^{b)}Electronic mail: alberto.zocante@uniupo.it

^{c)}Electronic mail: ove@chem.au.dk

I. ADDITIONAL FIGURES: WATER

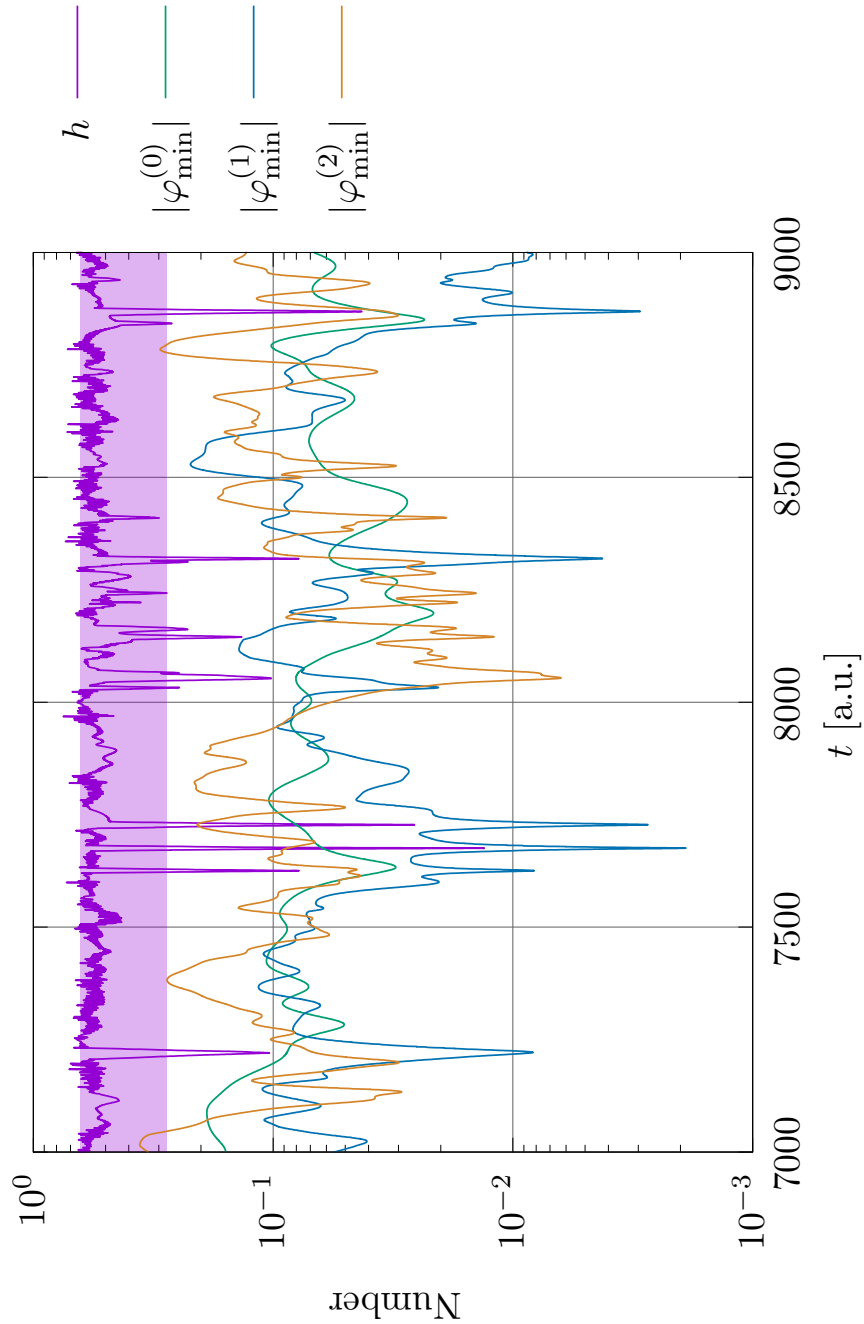


Figure S1. Integrator step size (h) and $|\varphi_{\min}^m|$ for the intramolecular vibrational energy redistribution (IVR) of water described at the TDMVCC[2] level using double exponentially parametrized modals ($\tau = 0$, i.e. no resets). The shaded area covers the mean step size plus/minus its standard deviation (computed within the shown time interval). Only part of the full time interval is shown for greater visibility.

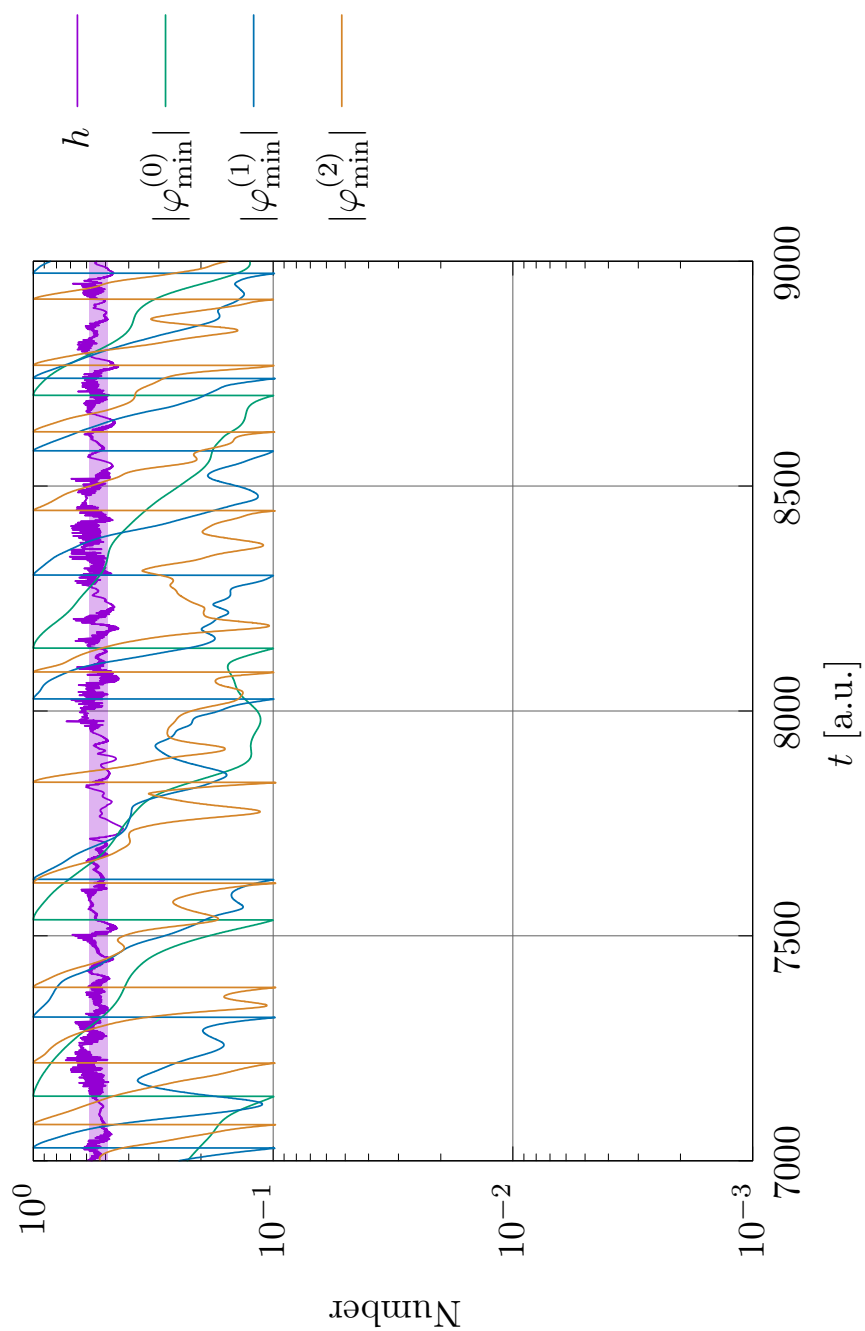


Figure S2. Integrator step size (h) and $|\varphi_{\min}^m|$ for the intramolecular vibrational energy redistribution (IVR) of water described at the TDMVCC[2] level using double exponentially parametrized modals ($\tau = 0.1$). The shaded area covers the mean step size plus/minus its standard deviation (computed within the shown time interval). Only part of the full time interval is shown for greater visibility.

II. ADDITIONAL FIGURES: 5D *TRANS*-BITHIOPHENE

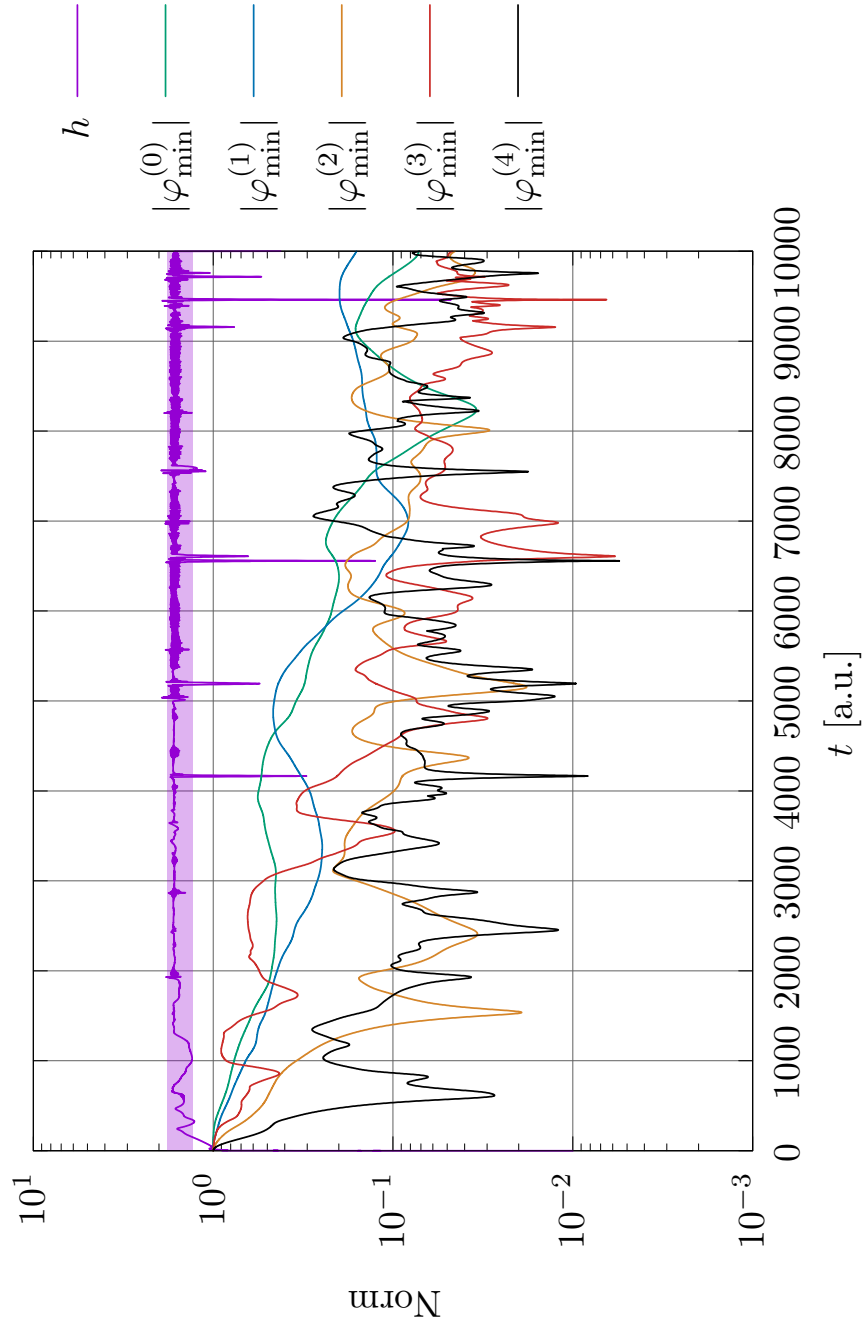


Figure S3. Integrator step size (h) and $|\varphi_{\min}^m|$ for the 5D *trans*-bithiophene model described at the TDMVCC[2] level using single exponentially parametrized modals ($\tau = 0$, i.e. no resets). The shaded area covers the mean step size plus/minus its standard deviation.

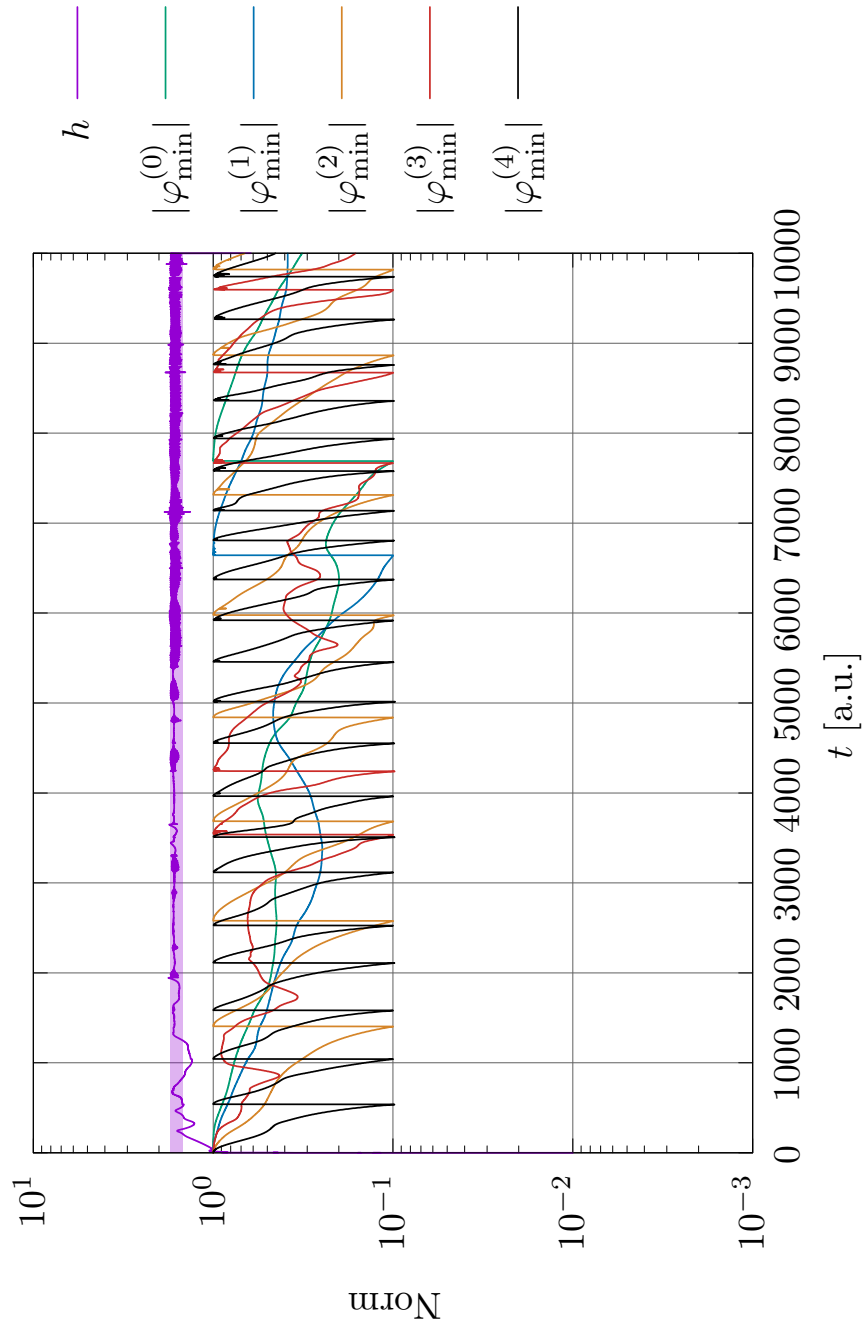


Figure S4. Integrator step size (h) and $|\varphi_{\min}^m|$ for the 5D *trans*-bithiophene model described at the TDMVCC[2] level using single exponentially parametrized modals ($\tau = 0.1$). The shaded area covers the mean step size plus/minus its standard deviation.